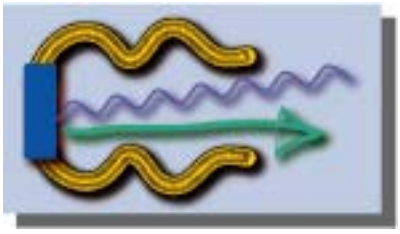

PHIN

Laser Temporal Pulse Shaping: Comparative Study Between LCM-SLM and DAZZLER Techniques

A. Ghigo[1], C. Vicario[1], M. Petrarca[2], S. Cialdi[3]

1) INFN-LNF, Frascati, Italy
2) INFN-Roma1, Rome, Italy
3) INFN Milano, Milan, Italy

Abstract

The generation of flat top pulse with 10 ps duration at 266 nm, is of extreme importance to achieve low emittance electron beam from a photoinjector. The production of this pulse shape is carried out using manipulation in the frequency domain with the aid of new programmable pulse shapers. In this paper we present the experimental measurements we performed to characterize two pulse shapers: the acousto-optics filter, namely the DAZZLER, and the liquid crystal mask spatial light modulator. The measurement have been performed with the amplified Ti:Sa laser system used to drive the SPARC photoinjector at LNF-INFN. The results obtained, the operation and the main limitations of the two techniques are also presented.

Introduction

The shaping of ultrafast laser pulses is of increasing interest in a wide variety of optical applications, including quantum and optimal control, high speed communications and material characterization. The promise of increasing the brightness of electron beams from RF (radio frequency) photoinjectors by using a flat top uv laser pulse to illuminate the cathode is the application inspiring the work presented here. For optimum driving a photocathode of a S-band RF cavity, such as the SPARC photoinjector, one desires ideally a relatively high energy (> 100μJ) UV laser pulse 5 to 10 picoseconds long, with a flat top temporal profile having fast ($\ll$1ps) rise and fall times [1–3]. The current techniques to manipulate the bell shape laser pulse employ devices that work in the IR, in general before the amplification. This set up requires the pulse shapers are able to compensate the unavoidable distortions caused by the amplification and the harmonic. To perform this pre-compensation is in general advisable to work with programmable shapers. We review here two most widespread techniques: one is based on a programmable dispersive acousto-optic modulator (the DAZZLER) while the other is based on a liquid crystal mask spatial light modulator (LCM-SLM) placed in a 4-f optical setup.
The described techniques are well-known but, according to our knowledge, the two pulse shapers have never been directly compared in the same experimental conditions. We present the performances of the two devices tested with the SPARC laser system.

The principle of laser pulse shaping in time domain is based on the amplitude and phase modulation of the spectral components. The field of a light pulse has, in the time and frequency domains, respectively, the expressions:

$$E(t) = \sqrt{I(t)}\, e^{i\Phi(t)} e^{-i\omega_0 t} \qquad \widetilde{E}(\omega) = \sqrt{\widetilde{I}(\omega-\omega_0)}\, e^{i\widetilde{\Phi}(\omega-\omega_0)} \qquad (1)$$

The pulse shaping manipulation is a linear filtering process. In the time domain the filter action of the shaper is represented by an impulsive response function h(t); in the spectral domain the filter action is represented by the Fourier transform H(ω) of h(t). The output electric field $E_{out}(t)$ is the convolution of the input $E_{in}(t)$ and the response function h(t): $E_{out}(t) = h(t) \otimes E_{in}(t)$. In the frequency domain we can write: $\widetilde{E}_{out}(\omega) = H(\omega) \cdot E_{in}(\omega)$.
In general H(ω) is a complex function that can be decomposed as an amplitude and phase terms: $H(\omega) = T(\omega) e^{i\phi(\omega)}$. Appropriate T(ω) and phase ϕ(ω) modulation can lead to any kind of output signal compatible with the original spectral width. When the input and output fields are given and it is possible to introduce both amplitude and phase modulation the solution of the problem is unique. This solution can be computed by using those particular functions T(ω) and ϕ(ω) that make the Fourier transform of the input equal into the Fourier-transformed output [4]. Nevertheless, in order to obtain the target pulse, it is possible to apply only an appropriate phase function modulation; in this case there are multiple solutions to the problem of find the filter transfer function[5].

Experimental setup

The experimental set-up used to perform the comparison between the two pulse shapers is reported in Fig. 1. Due to their low optical damage threshold and relatively high insertion

losses, the two devices are placed immediately after the Ti:Sa oscillator (central wavelength 800 nm, repetition rate 79.3 MHz and ~6nJ energy per pulse) before the CPA amplifier composed by a regenerative plus a multipass stage.

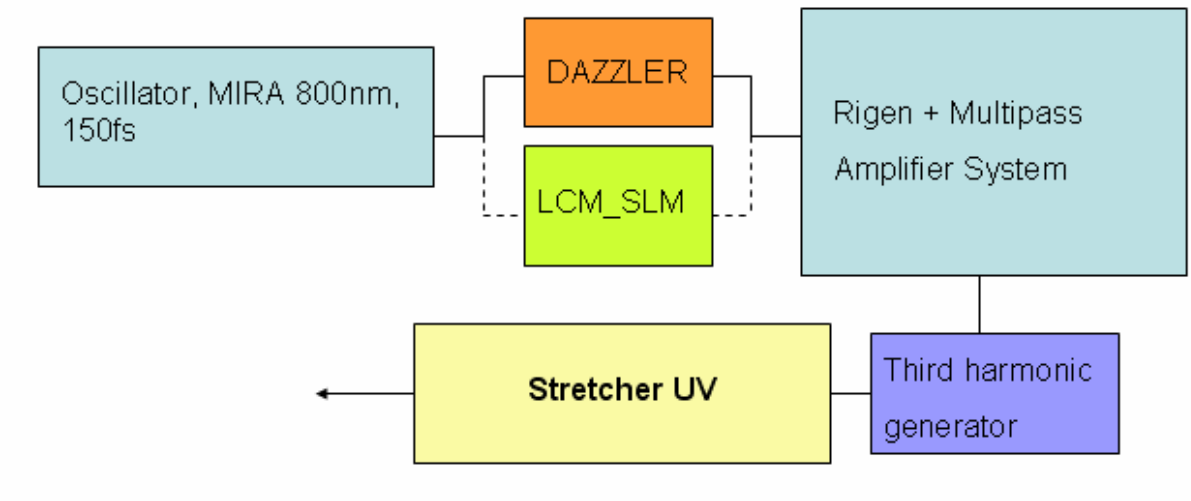

Figure 1: SPARC laser system; the two pulse shapers are easily interchangeable.

The amplification process is carried out by one regenerative pre-amplifier pumped by 7 W frequency doubled Nd:YLF laser and a two double passes stages which are excited by the second harmonic of a Nd:YAG with an energy of 0.5 J per pulse. The system delivers 100 fs pulses at λ=800 nm with energy of about 50 mJ and a repetition rate of 10 Hz.
At the output of the amplifier the IR pulses go to a third harmonic generator, where UV pulses with energy of up to 4 mJ are produced. The up-conversion is required to generate photon with energy larger than the photoemission work function of the metal cathode. The third harmonic generator is characterized by two type I beta barium borate (BBO) crystals of 0.5 and 0.3 μm used to produce first the second harmonic signal and then the third harmonic signal by frequency sum. At the end of the laser chain there is a stretcher based on a pair of 4350 groove/mm UV reflecting gratings that is used to stretch temporally the pulses up to 15 ps. The utility of a UV stretcher placed after the harmonic generation is motivated by two principal reasons:

1) The stretcher is necessary in order to maximize the third harmonic conversion efficiency obtaining the maximum UV energy on the cathode; in fact it allows us to temporally lengthen the UV pulses width after the harmonic conversion process whose efficiency depends on the input optical peak power. The IR pulse length at the entrance of the third harmonic generator does not change and therefore the harmonic conversion efficiency is independent on the laser pulse length desired on the cathode. Anyway IR pulse length variation can be controlled directly by the DAZZLER that is capable to broaden the pulse up to ~ 6 ps in the normal "single pass" configuration [6]. The LCM-SLM also permits to increase the IR pulse length, up to 10 ps. To stretch further the laser pulse the large phase variation over two neighbor pixels can causes diffraction effects.
2) The UV stretcher introduces a tight binding between the UV spectral and time profile of the laser pulses. In fact, as we have reported in [7-9], the spectral profile is transferred into the time profile due to the large chirp introduced by the stretcher. This consideration, obviously, simplifies the search of the optimal spectral phase and amplitude modulation. Moreover the direct correspondence time-spectral shape makes

straightforward the reconstruction of the pulse time intensity using a single shot high resolution diagnostic.

To measure the spectra at different wavelength we used an Ocean optics HR4000 spectrometer. For high resolution measurement of the UV spectrum we built a spectrometer based on a 4350 g/mm grating and f=30 cm lens. The wavelengths focused by the lens are recorded by a CCD camera assuring a resolution of 0.03 nm. The measurement of the time UV intensity is carried out by a multishot cross-correlator where a portion of amplified IR short pulse is mixed with the UV after the stretcher [11].

To find the optimal pulse shaper's phase and amplitude modulation to apply we developed the ORFEO code in Labview environment (see Fig. 2). This software tool calculates the second and third harmonic time profile and spectra starting from the measured fundamental harmonic spectral intensity. It is possible to apply an arbitrary spectral phase function and observe the changes on the harmonics time and wavelength intensities. The program includes also the distortions of possible non-linear crystals angular mis-alignment. Finally it is possible to simulate the linear chirp added with the UV stretcher.

The ORFEO code demonstrated to be useful and reliable tool and, it allows the direct comparison with the experimental data we presented in previous papers [9,13].

In the figure 2, the OEFEO screenshot is reported: the upper row from left to right shows the experimental IR spectrum, the second and third harmonic wavelength domain intensity. The lower row reports the corresponding calculated IR, blue and final UV time intensity. At the bottom, some knobs are noticeable; these visual inputs permit to synthesize the proper spectral phase function. The UV stretcher's chirp and the non-linear crystal angle deviation from the phase matching condition can also be simulated.

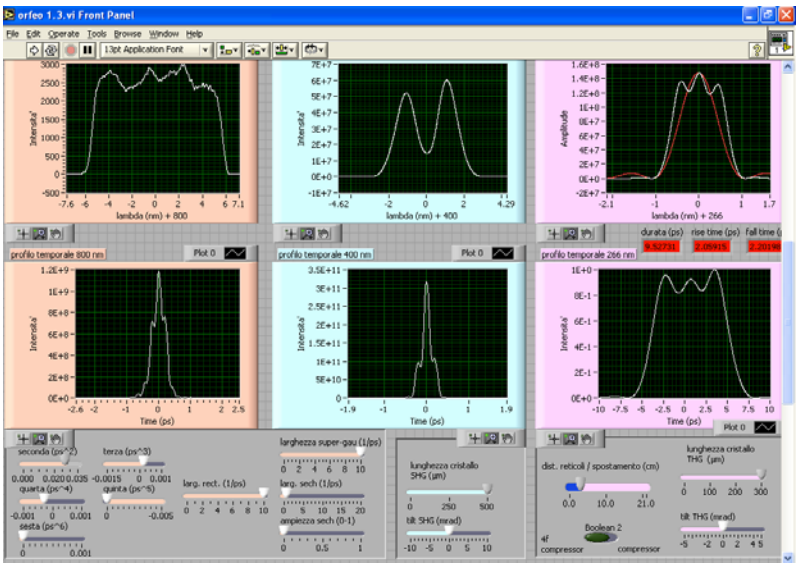

Figure 2: ORFEO code screen shot.

DAZZLER pulse shaper

The "DAZZLER", an "Acousto Optic Programmable Dispersive Filter", is a system designed by FASTLITE to manipulate the spectral phase and amplitude of ultrafast laser pulses [10].

A RF signal within 40−50 MHz excites a piezo transducer which generates an acoustic wave inside an bi-refrangent acousto-optic TeO_2 crystal. The acoustic wave propagates along the crystal spatially reproducing the RF signal. Being the optical wave velocity much grater than the acoustic wave velocity, the input optical pulse propagates as trough a fixed dielectric

grating inside the crystal. The two linear optical modes of the crystal can be efficiently coupled by an acousto-optic interaction when the phase matching condition, energy and momentum conservation, between the acoustic wave and the two optical modes are satisfied. The coupling condition assures a partial energy transfer from the input to the output optical mode. The two modes emerge out of the crystal at different angle and the part of the optical pulse interacted with the acoustic grating can be easily separated from the un-diffracted one, and then it can be amplified. The efficiency of the interaction for an optical wavelength depends on the amplitude of the corresponding acoustic frequency. Therefore by controlling the amplitude of the acoustic spectrum it is then possible to perform an amplitude modulation of the optical frequencies.

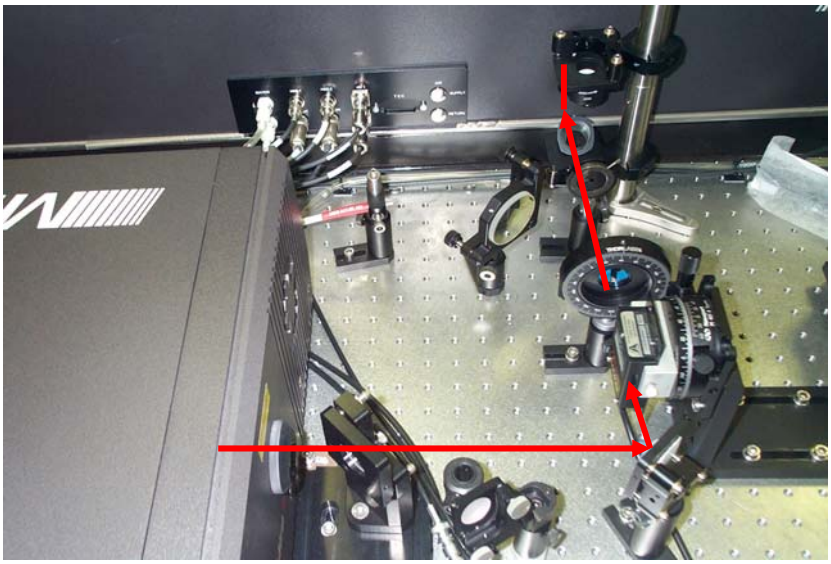

Figure 3: Dazzler set-up: the oscillator output is sent to the acousto-optic filter and a half wavelength wave-plate. After, a periscope is used to inject the beam in the amplifier.

Sending RF chirped signal in different position z along the crystal there will correspond different acoustic frequencies. Since locally, for a given z, there is just one spatial frequency in the acoustic grating, only the optical frequency that satisfy the phase matching condition, can be diffracted in that position z. In this way it is possible to diffract different frequencies at different depths. Due to the TeO_2 birefringence two wavelengths experience diverse propagation time and are subjected to different phase modulation.
The Dazzler we used is composed by a 2.5 cm acoustic material. It has a resolution of 0.3 nm and work over a bandwidth of 200 nm around 800 nm. The maximum chirp can apply produce a laser pulse up to 6 ps. The energy losses reach about 50 %.
As shown in the Fig. 3 the DAZZLER is mounted at the oscillator's exit and because polarization of the laser pulse is rotated by the acousto optic interaction, we use a lambda/2 waveplate prior to send the beam into the amplifier.
Our procedure to seek the flat top pulse is based on the search of the proper phase and amplitude modulation to obtain the target third harmonic spectrum profile that corresponds to the wanted time profile. As said before the target temporal pulse is obtained by generating a UV rectangular spectrum and then converting it into a rectangular temporal shape by the stretcher. To have the flat top spectrum at 266 nm we start generating a square-like spectrum after the DAZZLER and with proper amplitude modulation, pre-compensate the distortion introduced by the amplifier. In this way it is possible to have a flat top pulse out of the Hidra compressor.

As said before, it is not possible to produce directly 10 ps rectangular IR pulse before the harmonic generation because otherwise the conversion efficiency of the two BBO crystals would result too low. At the same time it is important to stress that it is not possible for the IR laser pulses to enter the crystals with temporal pulses that are too short.
In fact, the generated second harmonic and third harmonic spectral widths depend strongly on the first-harmonic pulse length [8, 9].

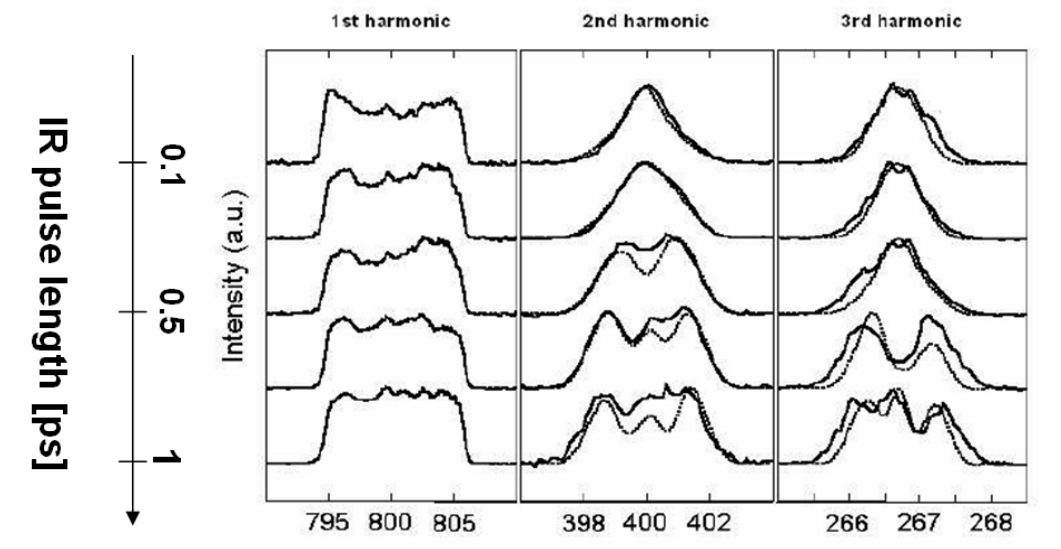

Figure 4: From left to right: measured (solid curve) and simulated with ORFEO (dashed curve) IR, BLUE, and UV spectra. Starting from a transform-limited pulse, we increase the

This behavior is shown in Fig. 4 by reporting the changes that occur in the spectrum of the second harmonic and third harmonic signals as a function of the chirp introduced by the DAZZLER. In the left part of the figure the first-harmonic spectra shaped by the DAZZLER are presented; the middle and the right parts show the experimental and calculated second harmonic and third harmonic spectra, respectively. Starting from a transform-limited pulse, we increase the chirp by 0.01 ps^2 for each curve from top to the bottom. As shown in the figure there are a good agreement between the measured spectra and the ones simulated by ORFEO. The DAZZLER phase function was set to have a IR pulse enough long, 0.7 ps, to preserve the flat spectrum trough the non linear crystals, and at the same time keep the third harmonic efficiency high. Using the amplitude modulation to have a flat top amplified IR spectrum and a proper phase modulation to keep the flat top spectral shape trough the third harmonic generator it was possible to have a reasonable square-like UV pulse in time. In the Fig. 5 is reported the UV pulse obtained with the DAZZLER shaper we measured with the multi-shot cross-correlator. The rise time obtained is about 2.6 ps and the oscillation on the plateau is limited to the 30% ptp. The oscillation takes into account also the shot-to-shot instability of 5% rms

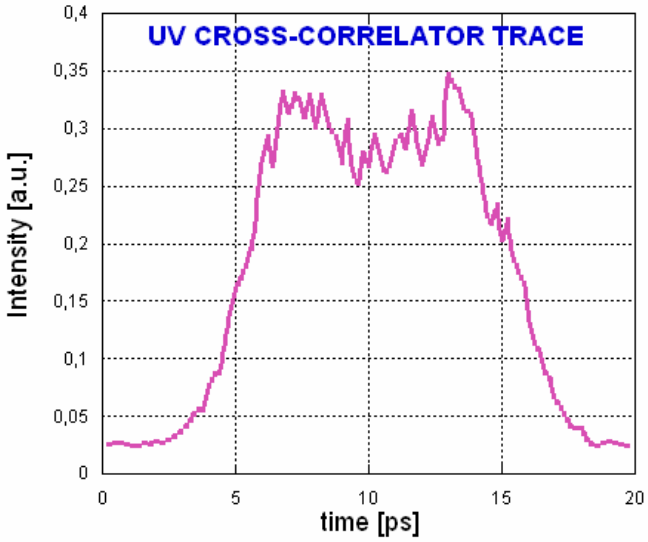

Figure 5: cross-correlation trace of the UV flat top pulse obtained with the DAZZLER pulse shaper.

LCM-SLM pulse shaper

We now discuss to operation principles of the pulse shaping system based on the LCM-SLM (liquid crystal mask – spatial light modulator).

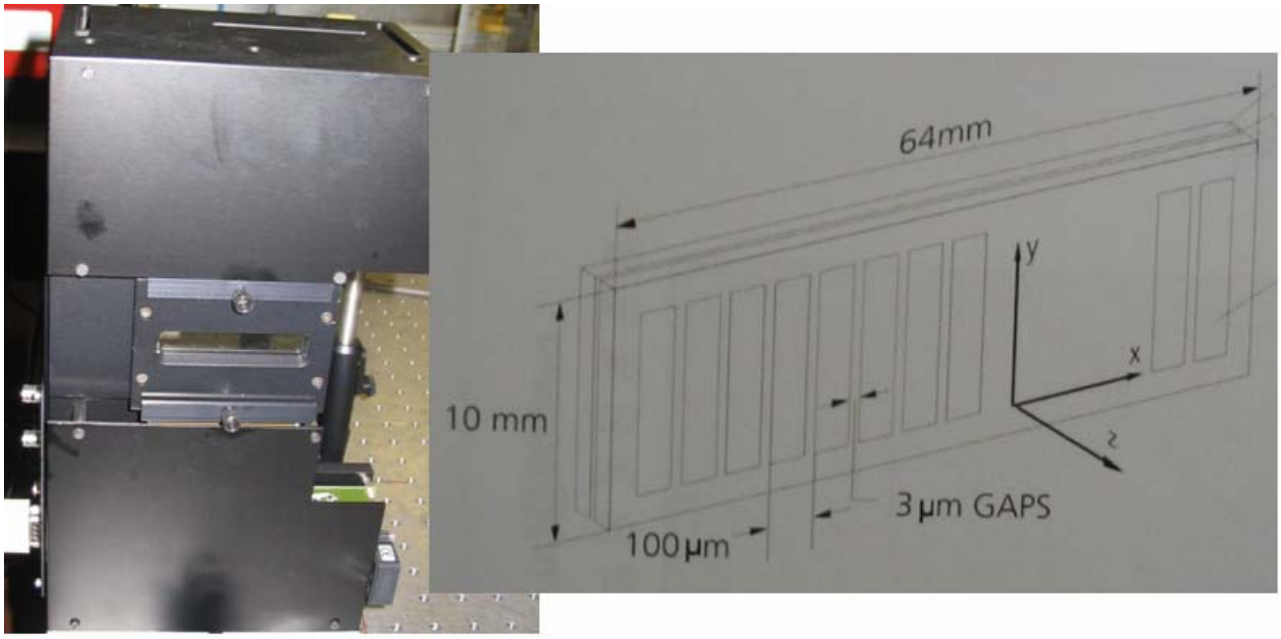

Fig. 6: Picture of the Jenoptick SLM-S 640/12 and on the right the sketch of the liquid crystal array.

The mask is an array of pixels interleaved with small gaps (Fig. 6). The mask chosen for the SPARC project is the Jenoptick model SLM-S 640/12. The dimensions of the pixels and gaps are, respectively, 97 and 3 μm wide, and the number of pixels is 640.
By changing the voltage applied to a single pixel it is possible to change the refraction index for that particular pixel. In this way, it is introduced a wanted phase shift in the radiation travelling trough the pixels. A LabView program has been developed in order to control the voltage applied to each pixel composing the liquid crystal mask.
The pulse shaping with the LCM-SLM is carried out introducing a proper spectral phase in order to obtain the wanted pulse intensity in the time domain.
In order to introduce the proper phase on the pulse it is necessary to propagate the different pulse wavelengths trough the individual pixels of the array. This is possible by using an optical layout called 4f which is reported in Fig. 7. The set-up is composed by two anti-parallel identical gratings and two focusing lenses with focal length f. The optical elements are placed as reported in the figure. The wavelengths are dispersed by the first grating, and then the first lens collimates the laser frequencies. The second lens and the last diffractive optics are used to recombine the wavelengths with no residual spatial chirp and without temporal dispersion. The mask is located at the Fourier plane of the system where the spectral components of the pulse are linearly dispersed and focused (see [4, 5]). The 4f layout shown in Fig. 8 has been designed to be compact in order to fit the space available on the optical table. The picture of the apparatus is shown in Fig. 9. The overall energy losses are comparable with the DAZZLER ones.

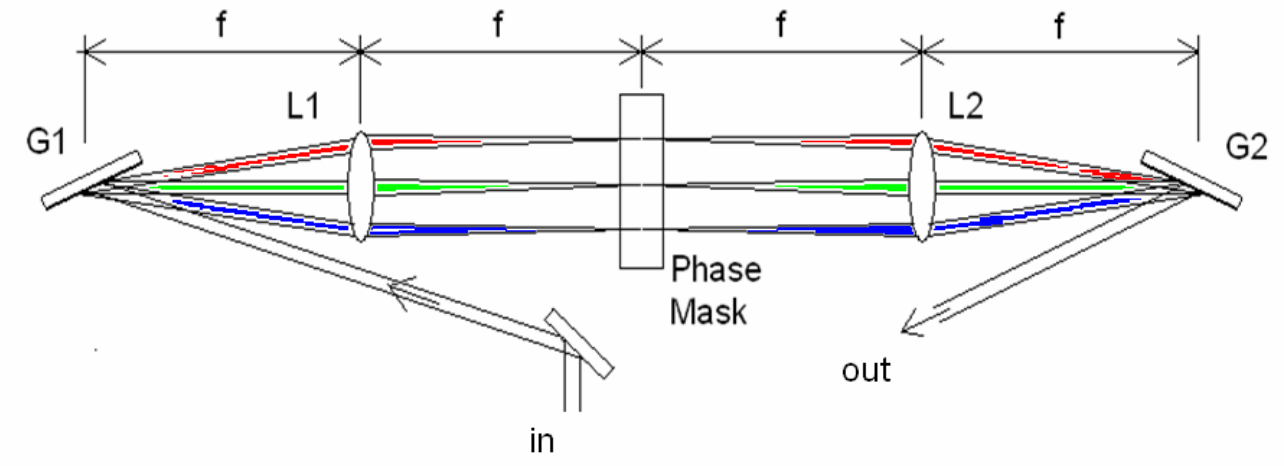

Figure 7 : 4f optical setup. The diffraction grating G1 is used in order to apply a linear angular dispersion onto the input wavelengths. L1 is used to focus the spectral component at the Fourier plane where the mask is placed. The second lens and the output grating are positioned in a symmetric position and are used to recombine the wavelengths at the exit.

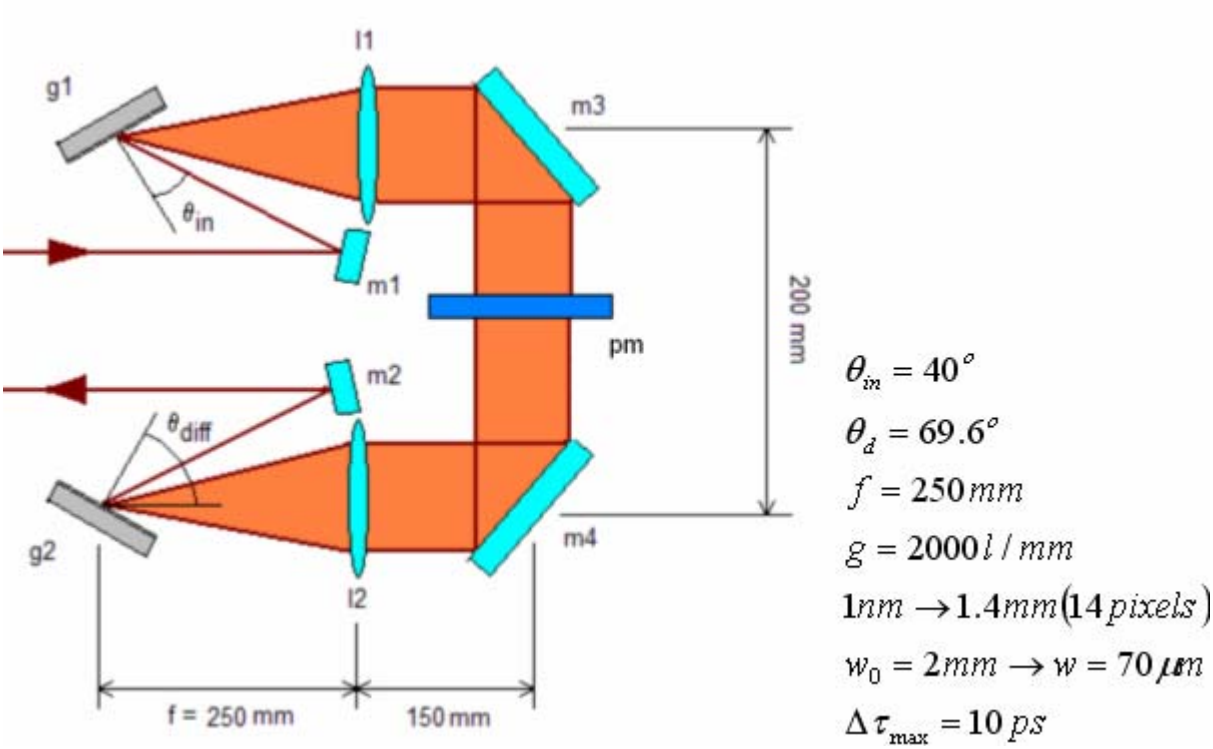

Figure 8: 4f optical setup implemented on the SPARC laser system

The phase function introduced by the mask and which is simulated is changed by modifying the coefficient of the following polynomial function

$$\phi(\omega) = \alpha \cdot (\omega - \omega_0) + \frac{1}{2}\beta \cdot (\omega - \omega_0)^2 + \frac{1}{3!}\gamma \cdot (\omega - \omega_0)^3 + \ldots$$

The first order coefficient "α" of the polynomial function brings a time shift of the pulse without changing its shape, the second order "β" induces a linear dispersion effect stretching or compressing the pulse and "γ" introduces a right or left asymmetry on the pulse shape. For our purposes the first four term of the polynomial function are sufficient.
The strategy that we studied and followed to obtain the results reported in this paper is based on the fact that, as said before, using the UV stretcher, the spectral profile can be converted into the time profile. We looked for a spectral phase modulation to introduce in the first harmonic pulse by the liquid crystal mask, capable to yield a third harmonic rectangular spectrum profile. The optimal phase function search was guided by the ORFEO simulations. In general a good strategy is to use the second order phase to enlarge the third harmonic bandwidth. At that point with the forth order phase we shrink the spectral tail and are able to make a square-like spectrum in the UV. The third order is used to compensate possible pulse spectrum asymmetry.

For the liquid crystal mask, the phase function modulation can be quickly introduced and it is possible to see in real time the changes of the UV spectrum. This characteristic makes this device suitable to be integrated with an adaptive algorithm as described in other paper [12].

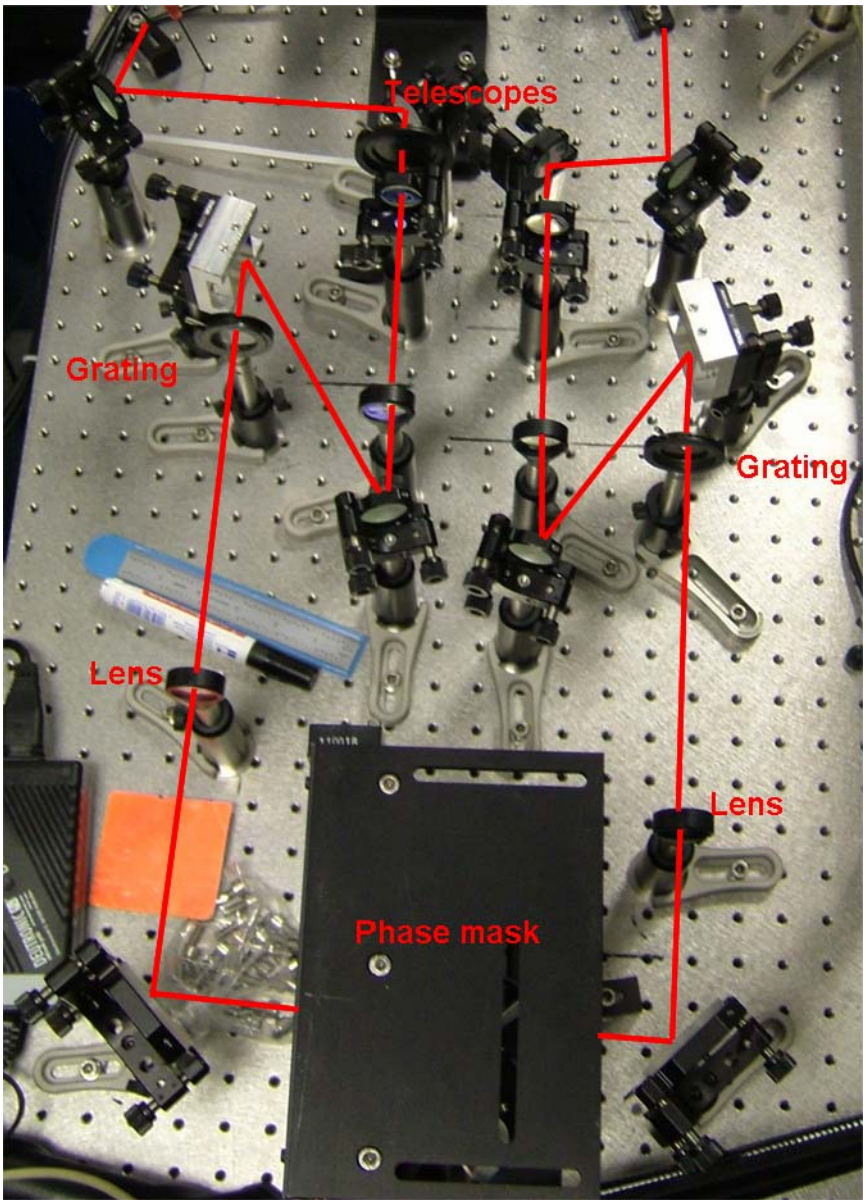

Figure 9: Picture of the 4f optical setup where is evidenced the optical path.

A critical point of LCM-SLM is the alignment of the system. In fact, it is not easy to perfectly align the 4f configuration in order remove any undesired effects such as spatial chirp and beam divergence of the output beam. This consideration is true especially when the optical setup is realized in small room, as in our implementation. The residual spatial chirp out of the 4f system is particularly deleterious since it seeds the regenerative laser. This amplifier is characterized by its own cavity's spatial and longitudinal modes. So, to avoid undesirable amplitude modulation of the amplified IR pulses, it is absolutely necessary that all the spectral components of the pulse coming out the 4f be well matched with the spatial modes of the RGA cavity. It is then clear that a diagnostic device for the IR before and after the RGA is mandatory to correctly align the 4f apparatus.
According to our experiences, when the chirp has been minimized out of the 4f setup it is important to accurately stir the regenerative input beam in order to produce an undistorted output spectrum out of the amplifier cavity. Anyway the output spectrum is very sensitive to even small misalignment of the seed beam and requires a real time control.

Once the alignment is done, the spectral amplitude is not influenced by the phase modulation and with the mask it is possible to control the IR manipulation up to the exit of the amplifier. Using the simulation code to take into account the alteration introduced by the third harmonic generation it was possible to achieve the flat top with 2.1 ps rise time. In Fig. 10 it is reported the cross-correlation trace of the UV pulse. The ripples on the plateau are enhanced by shot-to-shot amplitude fluctuations recorded during the measurement.

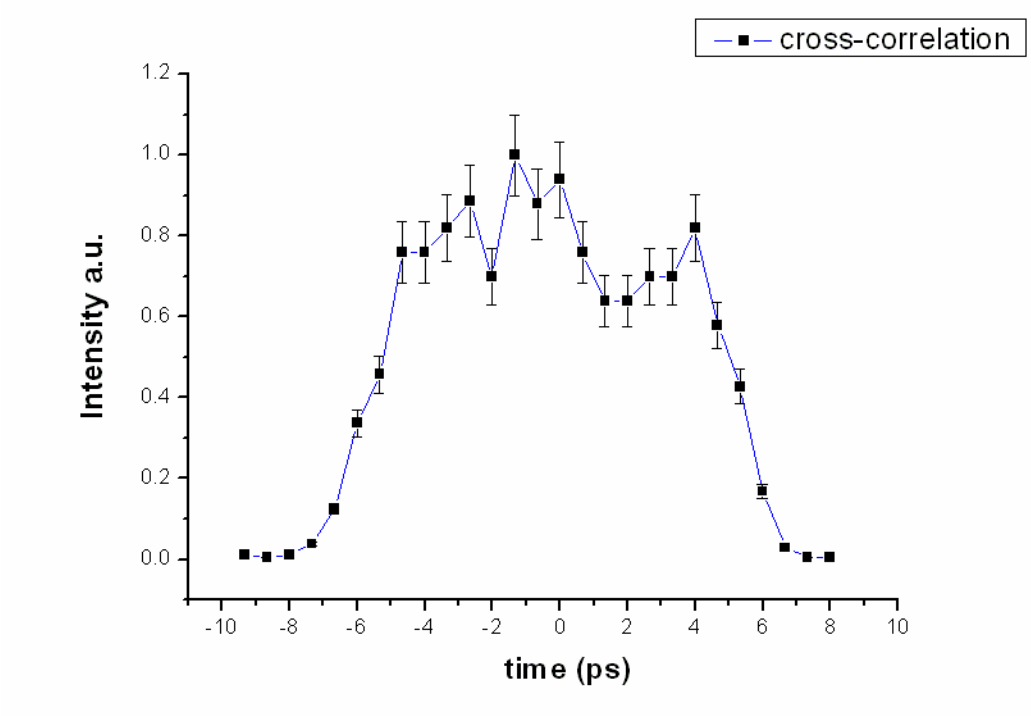

Figure 10: cross-correlation trace of the UV flat top pulse obtained with the LCM-SLM shaper.

We have also theoretically and experimentally verified that in order to manipulate the UV spectral profile by the phase function introduced in the fundamental, the bandwidth of the IR beam must not be too large (~10nm) otherwise the third harmonic spectrum starts to be excessively modulated by the BBO crystal bandwidth and it becomes difficult to introduce the desired phase modulations and reduce the rise time. To prevent this undesired effect in the Fourier plane we added two metal sheets to block the tails of the spectrum.

Discussion and conclusion

The shaping system based on the SLM is more complicated to be aligned with respect to the system based on the DAZZLER. For this reason the scheme 4f + SLM, from a maintenance point of view, is more critical also for the fact that the IR spectrum before and after the regen amplifier must be checked continuously.
The SLM requires to be found the calibration constant that allows converting the voltage applied to the single mask's pixel and the actual phase shift, between 0 and 2π, added to the optical wavelength.
Nevertheless the advantage of this scheme compared to the DAZZLER one is the better resolution and that the phase modulation can be introduced more quickly, therefore an iterative system can be simply implemented in order to find out the best modulation function.

This is basically what has happened in our case: using the DAZZLER we were not capable to obtain rise and fall time shorter that ~2.6 ps while with the SLM we obtained ~2.1ps for the same parameter values. We believed that this can be attributed to the smaller number of optimization attempts we did when the DAZZLER layout was used.
Anyway in both cases the rise and fall time is larger than 2 ps and we could not obtain faster edges. The reason for this is the smoothing effect on the UV spectrum due to the third harmonic generation process.
We have been capable to overcome this problem obtaining ~1.4 ps for the same parameter values by changing the shaping device system [13]. Summarizing, in the new shaping scheme, we sent the IR Gaussian spectrum into the amplifier without introducing any modulation in the IR. Then we used a modification of the UV stretcher to perform a cut of the UV pulse spectral tails. By controlling the cut sharpness it is possible to generate overshoot in the time profile that compensates the curvature that would correspond to a truncated Gaussian spectrum. This new scheme let us to simplify the all procedure to manipulate the pulses obtaining not only the target shape but also more exotic profiles as for example the multi-peaks.

Acknowledgements

We acknowledge the support of the European Community-Research Infrastructure Activity under the FP6 “Structuring the European Research Area” programme (CARE, contract number RII3-CT-2003-506395)

References

1. J. Yang, F. Sakai, T. Yanagida, M. Yorozu, Y. Okada, K. Takasago, A. Endo, A. Yada, and M. Washio, J. Appl. Phys. **92**, 1608 (2002).

2. L. Palumbo and J. Rosenzweig, eds., *Technical Design Report for the SPARC Advanced Photo-Injector* (Laboratori Nazionali Frascati, Istituto Nazionale di Fisica Nucleare, 2004).

3. P. R. Bolton and J. E. Clendenin, Nucl. Instrum. Methods Phys. Res. A **483**, 296 (2002).

4. S. Cialdi and I. Boscolo, Nuc. Inst. And Meth A 526 (2004) 239-248.

5. S. Cialdi, I. Boscolo, A. Flacco, J. Opt. Soc. Am. B 21, 9 (2004) 1693-1698.

6. C. Vicario et al. *Laser Temporal Pulse Shaping Experiment for SPARC Photoinjector,* Proceedings of European Particle Accelerator Conference, p. 1300, Lucerne, Switzerland, 2004.

7. S. Cialdi, I. Boscolo, Nuc. Ins. And Meth A 538 (2005) 1-7.

8. S. Cialdi, F. Castelli, I. Boscolo, Appl. Phys. B 82 (2006) 383-389.

9. S. Cialdi, M. Petrarca, C. Vicario, Opt. Lett. 31, 19 (2006) 2885-2887 and Virtual Journal of Ultrafast Science Oct. 2006.

10. F. Verluise, V. Laude, J. P. Huignard, P. Tournois, and A. Migus, J. Opt. Soc. Am. B **17**, 138 (2000).

11. M. Petrarca, C. Vicario, S. Cialdi, P. Musumeci, G. Gatti, A. Ghigo, and M. Mattioli, Rep. INFN-SPARC/LS-06/002 (INFN-SPARC, 2006). http://www.lnf.infn.it

12. S. Cialdi, I. Boscolo, A. Paleari, Report INFN/BE-05/02 October 10, 2005. http://www.infn.it

13. S. Cialdi, C. Vicario, M. Petrarca, P. Musumeci, Appl. Opt. 46, 22 (2007) 4959-4962.